

 Open access • Journal Article • DOI:10.1021/ACSCHEMNEURO.9B00264

Amyloid- β Peptide-Lipid Bilayer Interaction Investigated by Supercritical Angle Fluorescence. — [Source link](#)

Valentin Dubois, Diana Serrano, Stefan Seeger

Institutions: University of Zurich

Published on: 24 May 2019 - ACS Chemical Neuroscience (American Chemical Society (ACS))

Topics: Bilayer, Lipid bilayer, Peptide and Fluorescence spectroscopy

Related papers:

- [A comparative molecular dynamics analysis of the amyloid \$\beta\$ -peptide in a lipid bilayer](#)
- [Membrane-Accelerated Amyloid- \$\beta\$ Aggregation and Formation of Cross- \$\beta\$ Sheets](#)
- [Perturbation of membranes by the amyloid \$\beta\$ -peptide – a molecular dynamics study](#)
- [The two-fold aspect of the interplay of amyloidogenic proteins with lipid membranes](#)
- [Effect of the surface charge of artificial model membranes on the aggregation of amyloid \$\beta\$ -peptide](#)

Share this paper:    

View more about this paper here: <https://typeset.io/papers/amyloid-b-peptide-lipid-bilayer-interaction-investigated-by-1giysmr8e6>



**University of
Zurich**^{UZH}

**Zurich Open Repository and
Archive**

University of Zurich
University Library
Strickhofstrasse 39
CH-8057 Zurich
www.zora.uzh.ch

Year: 2019

Amyloid- Peptide–Lipid Bilayer Interaction Investigated by Supercritical Angle Fluorescence

Dubois, Valentin ; Serrano, Diana ; Seeger, Stefan

Abstract: The understanding of the interaction between the membrane of neurons and amyloid-beta peptides is of crucial importance to shed light on the mechanism of toxicity in Alzheimer's disease. This paper describes how supercritical angle fluorescence spectroscopy was applied to monitor in real-time the interaction between a supported lipid bilayer (SLB) and the peptide. Different forms of amyloid-beta (40 and 42 amino acids composition) were tested, and the interfacial fluorescence was measured to get information about the lipid integrity and mobility. The results show a concentration-dependent damaging process of the lipid bilayer. Prolonged interaction with the peptide up to 48 h lead to an extraction and clustering of lipid molecules from the surface and a potential disruption of the bilayer, correlated with the formation of peptide aggregates. The natural diffusion of the lipid was slightly hindered by the interaction with amyloid-beta(1-42) and closely related to the oligomerization of the peptide. The adsorption and desorption of Amyloid-beta was also characterized in terms of affinity. Amyloid-beta(1-42) exhibited a slightly higher affinity than amyloid-beta(1-40). The former was also more prone to aggregate and to adsorb on the bilayer as oligomer.

DOI: <https://doi.org/10.1021/acschemneuro.9b00264>

Posted at the Zurich Open Repository and Archive, University of Zurich

ZORA URL: <https://doi.org/10.5167/uzh-183309>

Journal Article

Accepted Version

Originally published at:

Dubois, Valentin; Serrano, Diana; Seeger, Stefan (2019). Amyloid- Peptide–Lipid Bilayer Interaction Investigated by Supercritical Angle Fluorescence. *ACS Chemical Neuroscience*, 10(12):4776-4786.

DOI: <https://doi.org/10.1021/acschemneuro.9b00264>

Amyloid- β Peptide-Lipid Bilayer Interaction investigated by Supercritical Angle Fluorescence

Valentin Dubois^a, Diana Serrano^a, and Stefan Seeger^a

^aDepartment of Chemistry, University of Zürich, Winterthurerstrasse 190, CH-8057 Zürich, Switzerland

ABSTRACT

The understanding of the interaction between the membrane of neurons and Amyloid- β peptides is of crucial importance to shed light on the mechanism of toxicity in Alzheimer disease. This paper describes how supercritical angle fluorescence spectroscopy was applied to monitor in real-time the interaction between a supported lipid bilayer (SLB) and the peptide. Different forms of Amyloid- β (40 and 42 amino acids composition) were tested and the interfacial fluorescence was measured to get information about the lipid integrity and mobility. The results show a concentration-dependent damaging process of the lipid bilayer. Prolonged interaction with the peptide up to 48 hours lead to an extraction and clustering of lipid molecules from the surface and a potential disruption of the bilayer, correlated with the formation of peptide aggregates. The natural diffusion of the lipid was slightly hindered by the interaction with Amyloid- β (1-42) and closely related to the oligomerization of the peptide. The adsorption and desorption of Amyloid- β was also characterized in terms of affinity. Amyloid- β (1-42) exhibited a slightly higher affinity than Amyloid- β (1-40). The former was also more prone to aggregate and to adsorb on the bilayer as oligomer.

Keywords: amyloid- β , Alzheimer, supported lipid bilayer, fluorescence, interface, supercritical angle fluorescence.

1. INTRODUCTION

Functions of proteins and polypeptide chains are intrinsically based on their three-dimensional structure. Whatever the structure is, it is reached in vivo in a short time scale after the synthesis of the molecule, driven by stabilizing non-covalent interactions between the amino acids^{1,2}. This process is referred to as protein folding. However, incorrect conformations might be the result of improper folding and be stable enough to hinder any restructuring toward the correct functional structure³. These “misfolded” polypeptides are likely to promote health troubles either by canceling necessary biological functions or gaining toxic properties⁴. Misfolded or disordered polypeptides sometimes aggregate into a specific structure called “amyloid fibril”. This amyloid fibril is characterized by a stack of β -sheet strands forming a cross- β structure perpendicular to the axis of fibril growth^{5,6}. Several diseases are correlated to the formation and deposition of such amyloid structure, either intra or extracellular^{5,7,8}. Among them, Alzheimer is a neurodegenerative disease of particular interest and is recognized by extracellular deposition of aggregated amyloid- β peptides (A β) as plaque composed of amyloid fibrils surrounding the neurons⁹.

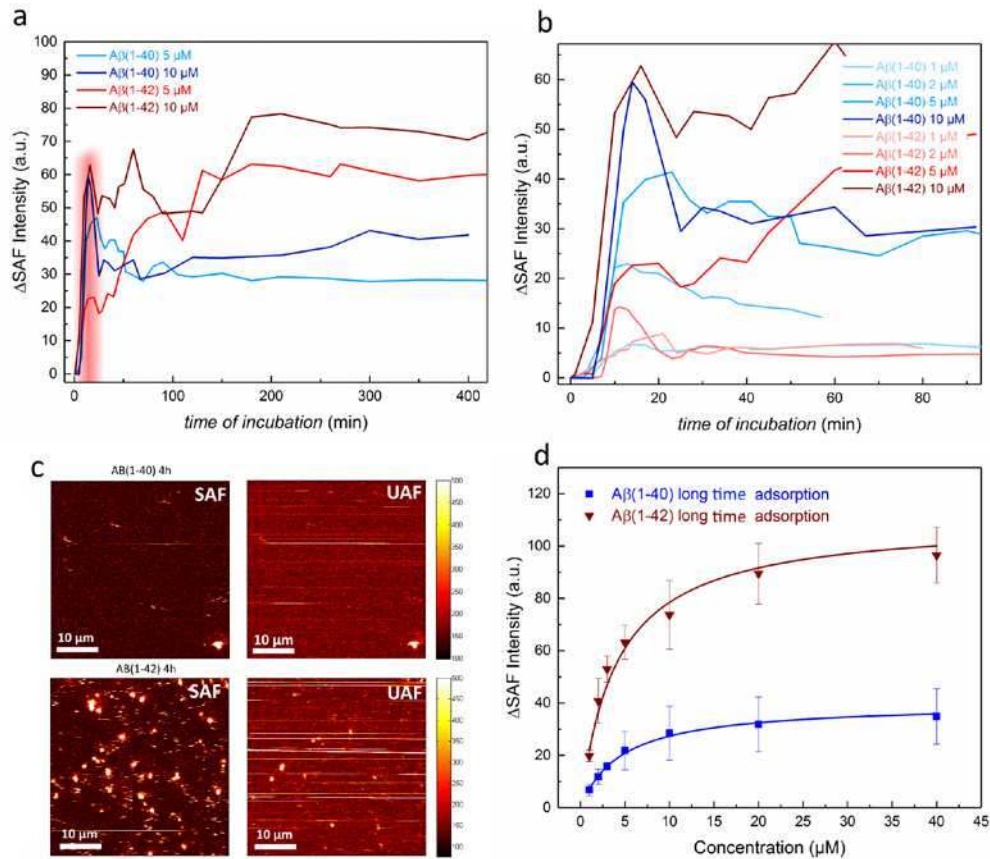
A β is a small peptide generated by the cleavage of a transmembrane protein called amyloid- β precursor protein (APP). The resulting A β fragments vary in their length but the most commonly found in Alzheimer plaque count 40 or 42 amino acids^{10,11}. The native structure of A β is usually described either as a random coil in aqueous solution¹² or as a small α -helix when interacting with membrane or hydrophobic surfaces^{13,14}. According to recent theories, the small oligomers formed in the early stage of aggregation are supposed to be more toxic for the neurons than the late fibrillar aggregates which constitute the extracellular plaque¹⁵⁻¹⁷. However, the direct cause for toxicity remains unclear. Different effects have been observed following the aggregation of the peptides and could explain the neuronal death encountered in the brain of disease patients. These effects include the oxidation of the lipid molecules in the membrane^{18,19}, hindrance of the lipids mobility within the bilayer²⁰ and formation of pore-like channels through the membrane of cells^{15,21,22}.

1 Different *in vitro* lipid structures have been established to study the impact of their interaction with peptides, assuming
2 that these models can partially mimic the response of neuron membrane *in vivo*^{23,24}. Among these models, supported lipid
3 bilayers (SLB) are planar fluid membranes formed by deposition and fusion of unilamellar vesicles (ULVs) onto
4 hydrophilic substrates²⁵. SLBs are easily formed on a support and are attractive due to their simplicity compared to cell
5 membranes. Furthermore, their formation takes place directly on an interface between the support and the sample medium.
6 This last feature makes the SLB model particularly suitable for surface sensitive techniques since the interaction with
7 peptides will occur only within this interfacial region. Supercritical angle fluorescence (SAF) is one of these selective
8 techniques. It allows to distinguish between fluorophores emitting a signal from the interface and those which are diffusing
9 in the bulk solution, without the need of any washing steps to remove unbound molecules. Therefore, real-time monitoring
10 of interaction processes is possible including recording kinetic data. This is achieved by specifically collecting the
11 fluorescence coming from above the angle of total internal reflection (critical angle) of a glass-water interface, essentially
12 emitted by the fluorophores situated near such an interface. Therefore, it excludes almost all fluorescence which is emitted
13 beyond a range of ~200 nm from the surface^{26,27}. In addition, undercritical angle fluorescence (UAF) can be collected
14 simultaneously. This signal corresponds to the output of a traditional confocal microscope. It allows to detect fluorophores
15 emitting from the bulk solution with a collection efficiency extending up to ~2.5 μm above the interface²⁸.
16 The simultaneous detection of SAF and UAF signal even allows the precise determination of the position of an emitter in
17 the axial direction from the surface, i.e. a precision down to a few nanometers. This technique has been already applied to
18 study the interaction of α -synuclein²⁹. SAF has also been developed for special fluorescence methods, e.g. SAF-FRET and
19 SAF-FCS³⁰. The SAF/UAF technique was used in this study to investigate the interaction between a negatively charged
20 SLB and two different A β 40 and 42 amino acids long peptides, referred to as A β (1-40) and A β (1-42) respectively. Among
21 these peptides, A β (1-42) was assumed to be potentially more toxic since it would have a higher propensity to aggregate
22 into oligomers³¹.

24 2. RESULTS AND DISCUSSION

25 2.1 Adsorption affinity of the peptides.

26 In a first experiment we studied in real-time the affinity of A β to SLBs by SAF. In order to quantify the early-stage
27 adsorption, non-fluorescent SLBs were incubated with fluorescently labelled peptide solutions (A β (1-40) and A β (1-42)).
28 Similar fluorescent labels were proven by Quinn et al. to yield analogous structures for aggregated A β and the unlabelled
29 peptides^{32,33}. Furthermore, in each sample only 1% of the peptides added were fluorescently labelled. Such amount limited
30 the influence of the label moieties on the aggregation of other peptides. It also prevented fluorescence self-quenching and
31 provided satisfying signal. Because the SAF channel only transmits photons arising from the interface, the signal was
32 considered as the emission of SLB-bound peptides only. The SAF signal was monitored over a certain area for different
33 peptide concentrations ranging from 1 μM to 40 μM during at least 6 hours after the beginning of the incubation. The
34 intensity of fluorescence was averaged over the complete area of each scan. The change in fluorescence intensity recorded
35 from the SAF channel was plotted as a function of the incubation time (Fig. 1 a). Results revealed a particular evolution
36 of the signal divided in two time-ranges. For an incubation time up to 30 minutes, all protein solutions showed a fast
37 increase in fluorescence intensity, followed by a systematic decrease in intensity. These results are interpreted as a fast
38 adsorption of the peptides followed by a partial desorption due to weak unspecific interactions. This behavior is well known
39 as “overshooting” and known also from the adsorption of other proteins³⁴⁻³⁷. This time range is hereafter referred to as
40 short-time adsorption (depicted by the red shade on Fig. 1 a). During the short-time adsorption, A β (1-40) displayed a
41 higher fluorescence signal than its more toxic counterpart A β (1-42) for concentrations between 1 μM and 5 μM (Fig. 1
42 b). However, this tendency was reversed beyond 10 μM , namely at concentration equal or superior to the critical micellar
43 concentration (cmc) of both A β 's³⁸. Around and beyond cmc range A β (1-42) is known to exist as higher order aggregates
44 than A β (1-40). This explains its subsequent higher fluorescence intensity during overshooting since the first adsorbed
45 peptides are bigger aggregates (cfr. supporting information, S1). Once the minima of SAF intensity have been reached
46 after the overshooting effect described previously, extended time of adsorption yielded in different behavior for each type
47 of peptide. A β (1-40) exhibited either a plateau or a slow increase when the time of incubation was prolonged beyond 24h.



1

2 Figure 1. Evolution of the SAF signal after incubation with fluorescent peptides. (a) Long-time adsorption of A β (1-40) and A β (1-42).
 3 Short-time adsorption is highlighted in red. (b) Short-time adsorption/overshooting period of A β (1-40) and A β (1-42). (c) Comparison
 4 between SAF/UAF imaging of 5 μ M A β (1-40) and A β (1-42) after 4 hours of incubation. (d) Maxima of fluorescence intensity after 6
 5 hours of incubation as a function of A β concentration.

6 On the other hand, A β (1-42) showed a further increase in fluorescence intensity after only one hour. A β (1-42) exhibits
 7 several irregular jumps of intensity before reaching another plateau. SAF imaging of the surface area allowed to correlate
 8 these fluctuations with the appearance of fluorescent aggregates on the SLB (Fig. 1 c). On the UAF imaging, bright stripes
 9 are visible which are attributed to the motion of these fluorescent aggregates in the bulk solution during the scanning
 10 process. Some of them will eventually adsorb durably on the interface and increase the SAF intensity. Also, some of the
 11 aggregates were less intense or seemingly absent from the UAF channel. This situation corresponds to fluorophores
 12 detected closer from the interface, whose fluorescence radiations are mostly sent above the critical angle²⁷. The part of
 13 their emission which is detected under the critical angle (UAF) is therefore smaller and they are harder to distinguish from
 14 the bulk fluorescence background. These fluorescent aggregates are thought to be the result of peptides oligomerization.
 15 As shown by the comparison of imaging between the two peptides, A β (1-42) exhibited a stronger and faster tendency than
 16 A β (1-40) to form these aggregates and nucleation sites of aggregation on top of the SLB after the short-time
 17 adsorption/desorption phase. This was especially obvious at concentrations above 5 μ M. This outcome is in accordance
 18 with previous reports showing the higher propensity of A β (1-42) to aggregate, due to the influence of the longer C-
 19 terminus³¹. Therefore, the outstanding signal of A β (1-42) on the interface after long-time adsorption could have three
 20 explanations. It was either due to the adsorption on the SLB of peptide aggregates pre-formed in solution ; or caused by
 21 peptides stacking on aggregates already adsorbed ; and/or simply caused by an enhanced adsorption of monomers due to
 22 a higher affinity for the lipids. The quantification of A β (1-40) and A β (1-42) affinities was required to assess this hypothesis.
 23 To quantify the affinity of the peptides for the SLB, the maximum of average intensity of the area after 6h of adsorption
 24 was plotted as a function of peptide concentration (Fig. 1 d). This curve was then fitted with a Langmuir isotherm³⁹

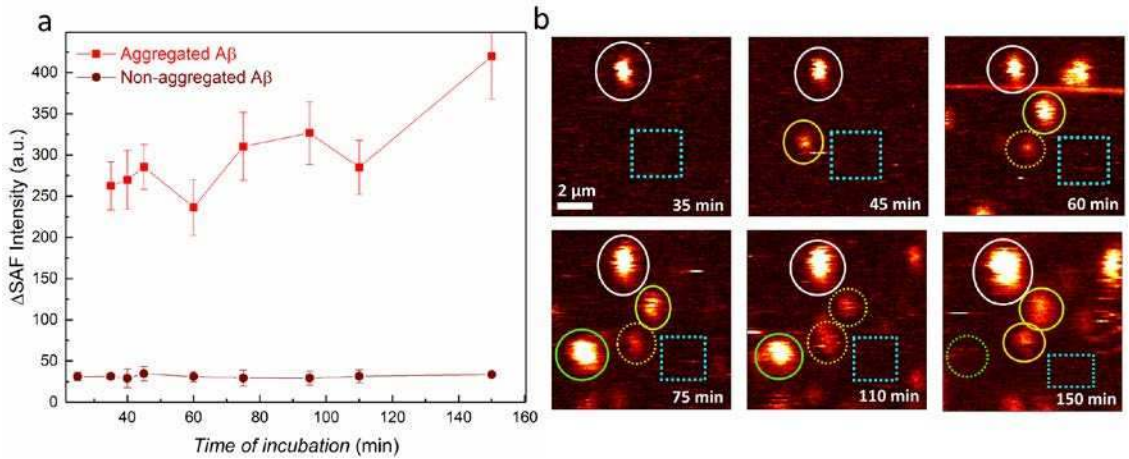
1 (Equation 1). Fitting yielded values for the unspecific adsorption constant (K_u), which were then expressed as dissociation
 2 constant (K_d) to quantify this affinity (Equation 2).

3

$$4 \quad I = I_{max} \frac{K_u \cdot c}{K_u \cdot c + 1} \quad (1)$$

$$5 \quad K_u = \frac{k_a}{k_d} = \frac{1}{K_d} \quad (2)$$

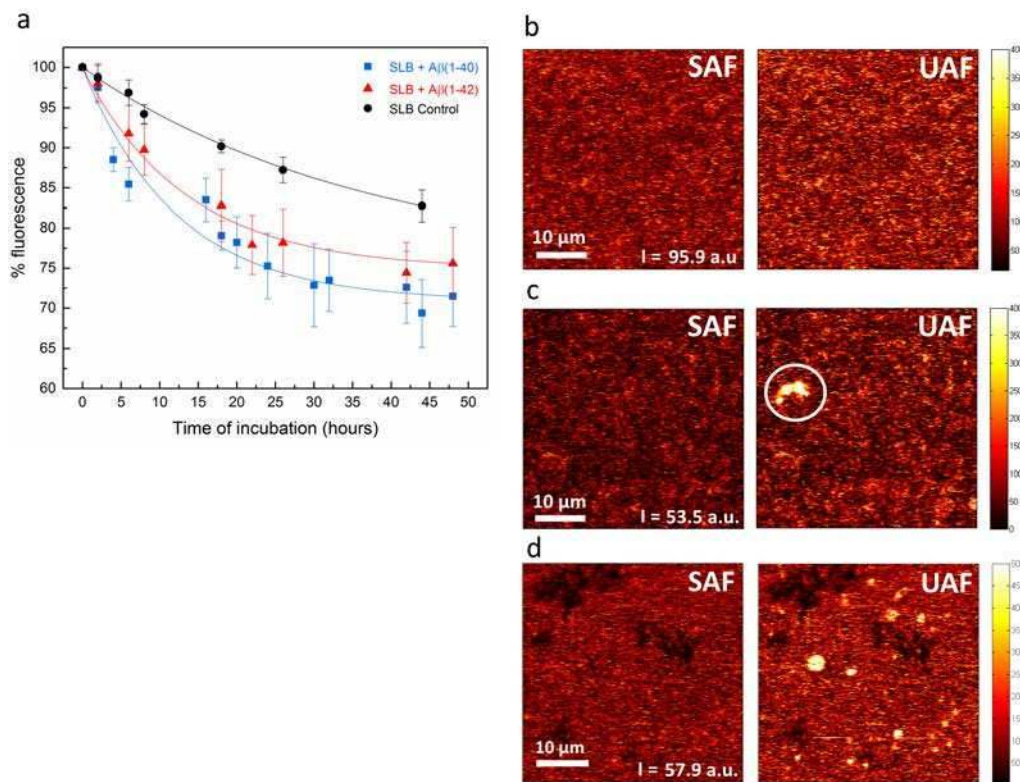
6 where I is the measured fluorescence intensity, I_{max} is the maximum fluorescence intensity reached at higher concentration,
 7 and k_a, k_b being the kinetic constants for unspecific adsorption and desorption respectively. The values calculated for K_d
 8 were $(4.24 \pm 0.28) \times 10^{-6}$ M for A β (1-40) and $(3.48 \pm 0.37) \times 10^{-6}$ M for A β (1-42). Despite the high limitation of the
 9 Langmuir isotherm model to describe protein adsorption events, the range of these values is in accordance with other
 10 studies^{40,41}. From these data, it is supposed that the slightly higher K_d value for A β (1-40) reflects a weaker interaction
 11 with lipid molecules than A β (1-42). This could be expected for the less toxic type of peptide, although the difference of
 12 affinity is too small to justify the discrepancies in SAF. Despite having similar values for K_d , the I_{max} of each peptide is
 13 drastically different, as shown in Fig. 1 c: the maximum SAF intensity of A β (1-42) is almost 3-folds higher than its
 14 counterpart. During these experiments, A β (1-42) reached a higher SAF intensity than A β (1-40) when aggregates became
 15 visible on the interface. From that moment, the SAF intensity increased until a plateau is reached, demonstrating that the
 16 aggregates are adsorbed durably and not reversibly. Since our results yielded a similar affinity of both peptides for the
 17 lipids, this increase of surface fluorescence is likely the consequence of the deposition and subsequent growth of these
 18 aggregates. More A β (1-42) adsorbed on the surface than A β (1-40) because they were in oligomeric state. So, the higher
 19 affinity of A β (1-42) for the SLB is nothing but a secondary factor to explain its higher SAF signal. The fact that A β (1-42)
 20 is the prior component of senile plaques in the brain^{42,43} supports the hypothesis that it aggregates more rapidly than A β (1-
 21 40) and interacts durably with the lipids at the early stage of the disease, while A β (1-40) is slower to oligomerize. In the
 22 absence of oligomers, the maximum adsorption of non-aggregated peptides is limited by the saturation of the surface with
 23 monomers. The adsorption of monomers is also reversible at least at the initial (overshooting) period (i.e. desorption is
 24 observed up to 30 minutes of incubation). This limitation would explain why a non-aggregating A β (1-40) peptide yielded
 25 less signal than A β (1-42), prone to form oligomers. To confirm this supposition, the evolution and average intensity of the
 26 non-aggregated A β (1-42) layer was selectively monitored and compared with the data obtained from its aggregates (Fig.
 27 2 a).



28
 29 Figure 2. (a) Evolution of SAF intensity as a function of time for non-aggregated layer and aggregated sample of 10 μM fluorescent
 30 Aβ(1-42). (b) SAF imaging data with the tracking of the aggregates over time displayed by colored circles (each colored circle
 31 correspond to one of the aggregates which remain at similar location). The SAF intensity of the first aggregate (white circle) and non-
 32 aggregated area (blue box) are displayed in (a).

1 From its constant SAF value, it is clear that the layer of adsorbed non-aggregated A β is in equilibrium and saturation,
 2 respectively, with the incoming flow of peptides once the surface is saturated. Moreover, the SAF intensity of the non-
 3 aggregated layer of A β (1-42) (Fig. 2 a, bottom line) is similar to the average SAF intensity of A β (1-40) in Fig. 1 a,c. This
 4 confirms that the presence of A β (1-42) aggregate is the main source for the discrepancies in maximum SAF intensity:
 5 without these aggregates, the two peptides would exhibit comparable SAF signal. Unlike the non-aggregated peptide areas,
 6 the fluorescent aggregates displayed in Fig. 2 b exhibited an increasing intensity. The aggregates are adsorbed tightly
 7 enough at the lipid bilayer so that most of them can be "tracked" by SAF imaging. This is represented in Fig. 2 b where
 8 each circle corresponds to the follow-up of one aggregate, a dashed circle indicating the same aggregate desorbs. They
 9 seemed to spread or desorb punctually, but the lateral position of many of them remained similar over a time-span of more
 10 than 2 hours. These measurements confirm the assumption that non-aggregated monomeric A β (1-40) and A β (1-42) have
 11 a similar adsorption affinity. The different adsorption behavior of A β (1-40) and A β (1-42) arises from the aggregates and
 12 not from the monomeric peptides. On the other hand, new interrogations came from the SAF imaging and tracking of the
 13 aggregates, whose motion seemed extremely limited. This might have been caused by an immobilization of the peptides
 14 on the glass surface, through the SLB. To check the latter hypothesis, the incubation of 10 μ M A β (1-42) on SLB or on a
 15 bare glass slide was compared (cfr. supporting information, S2, S3). The more static aggregates were observed on both
 16 surfaces. But on average, the fluctuation of the fluorescent clusters indicated that only few peptides were totally
 17 immobilized on glass or on SLB. Comparison between bare glass and SLB also showed a net preferential adsorption of
 18 peptides on lipids. Therefore, it seems reasonable to assume that alterations of the membrane are caused by these
 19 interactions rather than by artefacts from peptides adsorbed on the glass slide.

20 2.2 Impact of A β adsorption on fluorescently labelled SLBs.

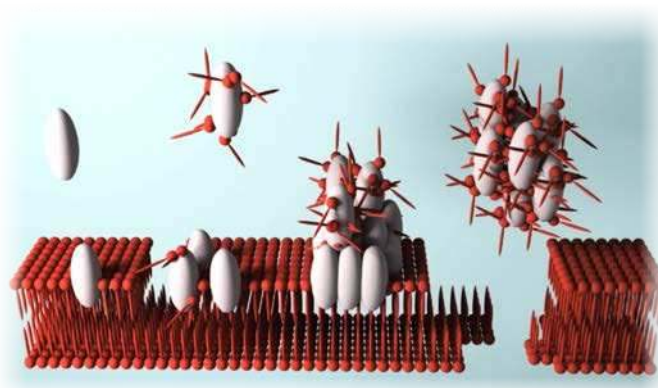


21

22 Figure 3. (a) Evolution of the SLB average fluorescence intensity over the time of incubation with 0.5 μ M A β solutions. (right side)
 23 Comparison between SAF and UAF imaging of SLB after 24 h of incubation (b) without peptides (PBS only), (c) with 5 μ M A β (1-40),
 24 (d) with 50 μ M A β (1-40). The average SAF intensity of the SLB is displayed at the bottom right corner.

1 To elaborate the impact of the A β adsorption on the SLB, the signal from a fluorescently-labelled SLB was monitored
2 upon incubation with unlabeled peptides. Typically, images of the bilayer were recorded periodically in both SAF and
3 UAF channels at different concentrations and at incubation times up to 48 hours. Three different effects could be observed,
4 depending on the concentration of peptides: a decrease of the average SLB fluorescence intensity; the formation of
5 fluorescent lipid aggregates; and eventually the disruption of the bilayer. At concentration between 0.5 and 5 μ M, both A β
6 (1-40) and A β (1-42) promote a decrease in SLB fluorescence intensity over time (Fig. 3 a). A lipid control confirmed that
7 this effect was not only due to photobleaching or natural damaging but indeed reflected an influence of the peptides.

8 When incubated with A β solutions of concentrations beyond 5 μ M, the imaging displayed some fluorescent aggregates,
9 attributed to the clustering of lipids (Fig. 3 c). The signal of these lipid clusters was more intense in the UAF than in the
10 SAF channel. This interesting feature can be explained by a protrusion of the lipids growing beyond the interface and the
11 maximum detection efficiency of SAF. Since the protocol for the formation of SLB (section 4.2) includes a washing of
12 most of the unbound lipid vesicles, lipids clusters cannot be due to residual vesicles and are more likely formed from the
13 interfacial lipids themselves which protrude above the bilayer. It is interesting to point out that the minimum A β
14 concentration for the formation of these lipid clusters coincide with the minimum concentration at which peptide
15 aggregates were observed (cfr. section 2.1). Therefore, this is an indication that peptide aggregation and lipid clustering
16 are two concerted events. Besides the clustering of lipids, the formation of small dark areas in the SLB could be observed
17 after approximately 20 hours of incubation with 50 μ M of peptides. Such dark areas are attributed to a local desorption of
18 the two lipid leaflets from the interface. These “holes” within the SLB had a diameter around 2-3 μ m. The formation of
19 smaller pores with a diameter size of 16 nm have been reported after 20 min for A β directly mixed with liposomes⁴⁴,
20 which is beyond the lateral resolution of the microscope used in this study (550 ± 50 nm). Longer monitoring showed the
21 holes spreading among the SLB and consequently resulted in a bilayer disruption. Beyond 24 hours of monitoring, a real
22 disruption of the bilayer could be observed (Fig. 3 d). From these results it appears that a part of the toxicity of the two
23 amyloidogenic peptides could arise from a progressive and concentration-dependent lipid removal process. The
24 interactions with the peptides can induce an extraction of some lipid molecules from the bilayer, resulting in a decrease of
25 fluorescence and thinning of the membrane when the lipid-peptide complex desorbs from the surface. These extracted lipid
26 molecules can cluster due to the aggregation process between peptides encountered at higher concentration, assuming that
27 each peptide maintains its interaction with extracted lipids while aggregating. At some point, the aggregated lipid-peptide
28 structures may become too massive and unstable to withstand the flow of solution inside the measuring cell, hence being
29 washed away and forming holes within the bilayer. These holes can eventually yield the disruption of the SLB (Fig. 4).
30 This hypothesis is in agreement with other theories despite the discrepancies in SLB compositions, affinities or steady-
31 state experiments within these studies^{20,29}.



32

33 Figure 4. Scheme of the hypothesized mechanism of toxicity of A β upon interaction with a lipid bilayer. A progressive and
34 concentration/aggregation-dependent lipid removal process leads to a thinning and potential disruption of the SLB

35

In addition, these results were observed with two different SLB compositions, one including cholesterol. The only difference observed was the strength of the lipid-desorbing effect (cfr. supporting information, S4). Although a concentration of 50 μM A β is physiologically irrelevant⁴⁵, lower concentration of the peptide also yielded a loss of fluorescence, which is still attributed to an extraction of lipid molecules. This effect could be sufficient to destabilize the structure of the membrane bilayer by reducing its thickness. Such event can hinder biological functions localized around the membrane and eventually promote cellular death.

2.3 Evolution of the diffusion coefficient of lipids in SLB.

Another important feature of lipid bilayers is the intrinsic mobility of lipid molecules and their lateral diffusion within the lipid leaflets^{46,47}. Fluorescently labelled SLBs were studied by supercritical angle fluorescence correlation spectroscopy (SAF-FCS) upon incubation with peptides, using the signal detected by the SAF channel (cfr. supporting information, S5). Correlation plots were then fitted with a 2-dimensional diffusion model. Fitting allowed calculation of the diffusion coefficient (D_L) which quantifies the lateral diffusion of lipid molecules (Equations 3, 4). Control values for SLB composition used in this study were in accordance with analogous data, considering discrepancies between the samples ($\sim 3\text{-}4 \times 10^{-12} \text{m}^2 \text{s}^{-1}$ for pure DOPC⁴⁸ and $\sim 2\text{-}3 \times 10^{-12} \text{m}^2 \text{s}^{-1}$ for DMPC⁴⁹). FCS data of SLBs were recorded using different concentrations of A β peptide (Table 1). Most of A β samples had small impact on the mobility of lipid molecules during our experiments. Even at concentration as high as 50 μM , A β (1-40) did not influence the lateral diffusion of the lipids apart from the vicinity of the bilayer disruption. A possible explanation is provided by Ding et al. and their results of fluorescence recovery after photobleaching (FRAP) experiments, showing that the two D_L values, of lipids and A β peptides respectively, were close⁵⁰. Similarity between the speed of diffusion of the lipids and A β would explain why the peptide has minor influence on the lateral diffusion of the SLB in our experiments. However, the more toxic A β (1-42) induced a significant drop of the D_L of our SLB at a concentration of 25 μM . In addition, A β (1-42) started to influence the diffusion of lipids after a minimum of 2 hours of incubation and it was known from previous results that after such a delay, A β (1-42) would likely have formed aggregates on the surface of the SLB (cfr. section 2.1). It is supposed that the more massive aggregated species were able to slow down the diffusion of the lipids while smaller peptide species previously adsorbed had no influence. The fact that only A β (1-42), with a higher propensity to aggregate, exhibited a general impact on the diffusion of lipids support the oligomeric hypothesis. This can be regarded as another proof of the oligomeric nature of toxic A β , since the condition for the hindrance of the lipids diffusion coincides with the formation and adsorption of aggregated peptide species.

Table 1. Values of the diffusion coefficient of SLB after 20 hours of incubation with A β peptide.

D_L ($10^{-12} \text{m}^2 \text{s}^{-1}$)	0.5 μM A β (1-40)	5 μM A β (1-40)	50 μM A β (1-40)	0.5 μM A β (1-42)	5 μM A β (1-42)	25 μM A β (1-42)
Before incubation	2.88 \pm 0.22	2.78 \pm 0.27	2.91 \pm 0.11	2.94 \pm 0.42	2.69 \pm 0.15	2.95 \pm 0.38
After 20 h incubation	3.01 \pm 0.10	3.06 \pm 0.07	3.14 \pm 0.05	2.91 \pm 0.40	2.43 \pm 0.06	1.90 \pm 0.18

2.4 Evolution of the diffusion coefficient of A β peptides.

In addition to the mobility of the lipids, the diffusion of A β adsorbed at the SLB surface was also measured with fluorescent peptides. The data resulting from the SAF-FCS experiments were fitted to extract the diffusion coefficient. However, the diffusion of A β is not limited to the surface. In addition to a lateral diffusion on the surface of SLB, the motion of peptides also includes their adsorption and desorption from the surface. Therefore a 2-dimensional diffusion model was insufficient to evaluate their diffusion properly. Instead, a SAF-3-dimensional model was used. It was elaborated to include the exponential decay of detection of the supercritical angle technique along the axial axis³⁰ as the peptides diffuse away from the interface. At a concentration of 5 μM the average diffusion coefficient of A β (1-40) was $(24.85 \pm 5.59) \times 10^{-12} \text{m}^2 \text{s}^{-1}$ while A β (1-42) had an average diffusion coefficient of $(2.79 \pm 0.49) \times 10^{-12} \text{m}^2 \text{s}^{-1}$. It appears that the diffusion coefficient of A β (1-42) is in the range of the D_L calculated for the SLB (table 1) while A β (1-40) diffused faster by one order of magnitude. A β (1-42) was previously identified as the peptide with a higher affinity for SLB and was adsorbed more tightly, therefore it could be appropriate that this peptide and the lipids diffuse with a similar speed. On the other hand, A β (1-40)

1 is less tightly adsorbed and the amount of peptides within the detection volume fluctuates more rapidly due to faster
2 adsorption/desorption processes. Quantitative comparison between the D_L of the lipids and D_L of A β should be made
3 carefully since a 2-dimensional model was used to fit the diffusion of SLB, in contrast with the 3-dimensional SAF model
4 used to fit the diffusion of A β . A simple qualitative analysis between the two types of peptide is more relevant, yet it shows
5 explicitly that the SAF intensity of A β (1-42) fluctuates less than its shorter counterpart, hence the lower D_L for A β (1-42).
6 The major contribution to the fluctuations of intensity is attributed to the adsorption/desorption process inside and outside
7 of the detection volume, rather than a lateral diffusion at the surface of the bilayer. Discrepancies of this
8 adsorption/desorption process between the two peptides can be explained by the difference of affinity for the SLB and the
9 stability of peptide aggregates described in section 2.1. The FCS data obtained show a relation between the number of
10 fluorescent emitters and the diffusion rate. Namely, A β (1-42) FCS data suggested a higher number of fluorophores than
11 the signal observed from A β (1-40) in the monitored areas (cfr. supporting information, S6). Therefore, the slower diffusion
12 of A β (1-42) correlates with a higher density of peptides on the surface, hence higher-order oligomers.

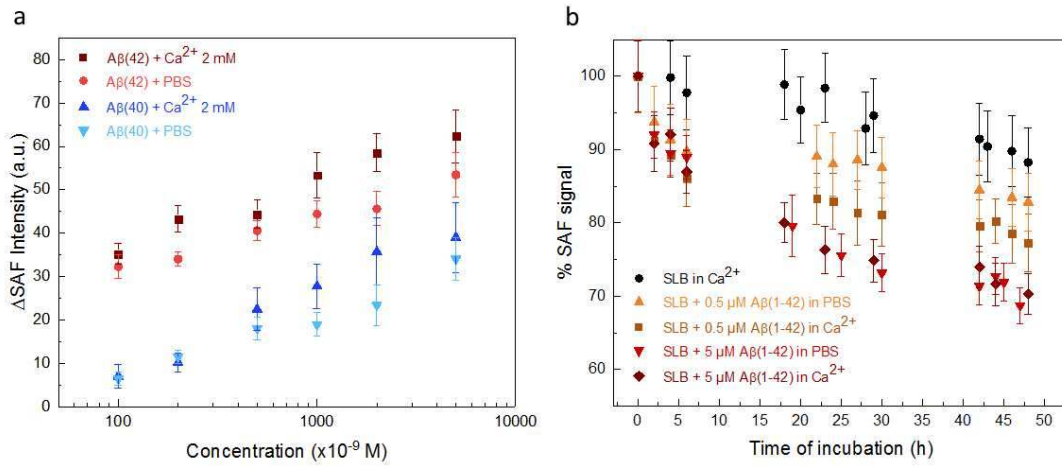
13 2.5 Influence of calcium ions on the interaction between A β and SLB.

14 The probable bidirectional relationship between A β and Ca²⁺ in Alzheimer disease has long been hypothesized⁵¹. A β can
15 disturb Ca²⁺ homeostasis⁵², notably by formation of cation-selective channels, as mentioned earlier^{53,54}. On the other hand,
16 dysregulation in the dynamics of Ca²⁺ ions can modify the brain metabolism and trigger the release of A β peptide⁵⁵.
17 Interactions between A β and Ca²⁺ also promotes the formation of oligomeric species⁵⁶ and facilitates the binding of the
18 peptide on the membrane⁵⁷ via formation of ionic bridges. For all these reasons, the experiments described in previous
19 sections have been repeated using PBS with 2 mM of CaCl₂ · 3H₂O. The obtained results have been compared with those
20 including A β dissolved in PBS.

21 First, the monitoring of the adsorption of A β dissolved in membrane buffer was reproduced at low concentrations on a
22 SLB. The average fluorescence of the monitored area was measured after 24 hours of incubation with the peptides. As a
23 matter of fact, dissolution in membrane buffer increased the number of adsorbed peptides on SLB, compared with peptides
24 dissolved in PBS (Fig. 5 a). This effect is thought to be the consequence of the interactions between A β and calcium ions.
25 Computational studies explain this effect by the formation of the previously mentioned ionic bridge. Ca²⁺ is supposed to
26 act as a link between the polar head group of the lipids and the peptides, negatively charged at neutral pH⁵⁸. It also
27 strengthens the electrostatic interactions between charged residues of A β and the SLB⁵⁹. Ca²⁺ also enhanced the amount
28 of aggregated species on the surface, even at concentrations as low as 200 nM (data not showed). This enhancement of
29 peptide aggregation can be expected since the ion-bridge can also occur between two negatively charged peptides. However,
30 the increase of fluorescent adsorbates due to calcium is only partially maintained beyond 2 μ M peptides. A β (1-40)
31 exhibited the highest enhancement of adsorption at concentrations of 1 and 2 μ M, while A β (1-42) adsorption was only
32 slightly strengthened at 5 μ M. It is expected that beyond 2 μ M, the concentration of peptides is sufficient for aggregation
33 to occur in PBS solution without the influence of ion-bridge between A β . Therefore, the influence of aggregation on
34 fluorescence intensity is not specific of Ca²⁺ buffer anymore. It is thought that the presence of Ca²⁺ can trigger the
35 aggregation of A β and act as a bridge between the peptides and the lipid bilayer. However, the influence of this bridging
36 effect on the adsorption is preponderant only at concentrations lower than 2 μ M. Beyond this limit, the flux of peptides
37 coming from the bulk solution toward the membrane is supposed to overcome the influence of the calcium.

38 Furthermore, Ca²⁺ enhanced the decrease in the fluorescence of SLB observed when interacting with the peptides at 0.5
39 μ M (Fig. 5 b). This outcome has several possible explanations. As Ca²⁺ triggers the oligomerization of A β peptide at low
40 concentration, it may promote more damaging within the SLB. Additionally, dynamic simulations showed that calcium
41 ions stimulate a deeper insertion of A β inside the bilayer⁵⁹, which correlates with a stronger disordering or thinning
42 effect^{60,61}. Another explanation is based on the previous conclusion that lipid removal is a concentration-dependent process.
43 Since calcium ions increase the amount of adsorbed peptide – aggregated or not - the amount of extracted lipid molecules
44 would be increased as well. Nevertheless, a conclusion similar to the previous adsorption experiment was drawn when the
45 concentration of peptide was increased to 5 μ M. At this concentration, the adsorption and aggregation features of A β were
46 almost identical when dissolved in PBS or Ca²⁺ buffer, therefore the impact of the peptide on the SLB did not differ either,
47 no matter in which buffer the peptide was dissolved. Finally, the influence of the peptide on the mobility of the lipid was
48 measured by FCS. The values of D_L of the lipids after incubation with the peptide in the Ca²⁺ containing liquid phase are

1 close to those obtained when A β is dissolved in PBS (Table 2). It was concluded in section 2.3 that the aggregation state
 2 of the peptides interacting with the SLB was the critical parameter to influence the diffusion of the lipids. The propensity
 3 to aggregate of such highly concentrated peptides interacting with the SLB seemed unaltered by the presence of Ca²⁺ ions,
 4 therefore no further reduction of the diffusion coefficient of SLB should be expected, as showed by the experiment.



5
 6 Figure 5. (a) Comparison of the adsorption of labelled peptide incubated over SLB in PBS and with Ca²⁺. (b) Comparison of the decrease
 7 in fluorescence intensity when labelled SLB are incubated with A β in PBS and with Ca²⁺.

8 Table 2. Comparison of the diffusion coefficient of lipids inside SLB incubated with A β (1-42) in PBS and Ca²⁺.

D_L ($10^{-12}m^2s^{-1}$)	5 μ M A β (1-42) (in PBS)	25 μ M A β (1-42) (in PBS)	5 μ M A β (1-42) (+ 2 mM Ca ²⁺)	25 μ M A β (1-42) (+ 2mM Ca ²⁺)
Before incubation	2.69 ± 0.15	2.95 ± 0.38	2.78 ± 0.20	2.81 ± 0.32
After 20 h incubation	2.43 ± 0.06	1.90 ± 0.18	2.39 ± 0.17	2.04 ± 0.22

9
 10 **2.6 Conclusion.**

11 In the present study the interaction between a lipid bilayer and two variants of A β peptides, responsible for Alzheimer
 12 disease, and also the effect of this interaction on the lipid molecules were investigated. Supercritical angle fluorescence
 13 microscopy was used in order to limit the detection volume to an area close to the bilayer interface. First, the adsorption
 14 of the peptides on SLB was monitored. From these results, the affinity of each could be calculated. Due to the absence of
 15 specific receptors in the bilayer, the interactions were considered as unspecific. As a matter of fact, the calculated values
 16 for K_d were in the range of low affinity interactions. A β (1-42) seemed to have a slightly higher affinity than the less toxic
 17 A β (1-40) after an incubation of a few hours, but mostly exhibited a higher tendency to form aggregates upon the bilayer.
 18 Further, the impact of such interactions on fluorescently labelled SLBs have been evaluated. Different effects were
 19 observed, depending on the concentration: a decrease of fluorescence intensity, a clustering of lipid molecules and
 20 eventually the progressive disruption of the bilayer. These effects were independent of which type of A β was incubated
 21 with the SLB. Despite the fact that these results were obtained with high concentration of peptides, they give an insight in
 22 the process which locally reduces the thickness of the bilayer and can make the cell membrane more fragile or even porous
 23 (Figure 4). The last step consisted to elaborate the effect of the peptides on the lateral lipid diffusion within the bilayer.
 24 A β (1-40) seemed to have no effect at all, while high concentration of A β (1-42) lead to a decrease in the mobility of lipids.
 25 Since the time of incubation, the concentration and the type of peptide required to affect D_L of lipids all coincided with
 26 the conditions for maximum aggregation of A β , it seems that the hindrance of the diffusion of lipids is correlated with the
 27 adsorption of massive oligomeric species. Saturation of the surface with monomers or small oligomers (Fig. 2 b) seemed

1 unable to affect the diffusion of the lipids. The diffusion of the peptides themselves is also a critical parameter, since only
2 the slowest diffusing peptide A β (1-42) affected the diffusion within the SLB.

3 In order to study the impact of calcium ions on these effects, experiments were repeated with A β (1-42) dissolved in a
4 buffer containing 5 mM of Ca²⁺ instead of PBS. The results confirmed previous computational studies which reported an
5 enhanced adsorption of the peptide on the lipids, probably due to the formation of ionic bridges, stronger electrostatic
6 interactions and oligomerization. Calcium ions also increased the loss of fluorescence of labelled SLB incubated with A β .
7 It was concluded that Ca²⁺ activates the toxicity of the peptide at low concentration, either by inducing oligomerization or
8 through a deeper insertion within the bilayer. It would be interesting to investigate the latter effect by the use of neutron
9 reflectometry. However, Ca²⁺ buffer did not yield any difference compared to PBS once the A β concentration was equal
10 or superior to 5 μ M and did not affect the influence of the peptide over the diffusion of the lipids at all. This result suggests
11 that the aggregation process of the peptides was unchanged by Ca²⁺ beyond 5 μ M. Therefore, the influence of Ca²⁺ in our
12 experiments was limited at low concentration of peptides for which calcium actually increased the amount of adsorbed
13 peptides, their aggregation and the potential disordering of the SLB. The influence of Ca²⁺ was lost once the concentration
14 of peptide was high enough to yield aggregation in PBS. Higher damaging of SLB, correlated with aggregation at low
15 concentration is another proof of the role of oligomers in the toxicity of A β . Eventually, the first stages of Alzheimer
16 disease could correlate with the interactions of low concentrated A β with Ca²⁺ near the membrane of neurons. Since the
17 toxic effects of the peptide disturb calcium homeostasis and the ions themselves trigger peptide release and adsorption, it
18 could be a progressive degenerative cycle.

19 3. METHODS

20 3.1 Setup design

21 A custom-made microscope objective was used to split the collected fluorescence arising from angles higher and lower
22 than the critical angle. For a glass-water refractive index discontinuity, this critical angle (θ_c) is 61°, according to the
23 formula $\theta_c = \arcsin(n_{\text{water}}/n_{\text{glass}})^{62}$. Therefore, the objective is designed with an internal parabolic shaped lens able to collect
24 radiation coming from above θ_c for aqueous sample or solution with the same refractive index than water ($n = \sim 1.33$).
25 Undercritical angle light is transmitted through a collection of lenses whose numerical aperture is equal to 1.0, which is
26 also used to focus the excitation light. The custom-made objective is mounted on an inverted Olympus IX71. The excitation
27 light source is a power tunable diode laser emitting at 633 nm (TOPTICA iBeam Smart). Optical parts are assembled to
28 drive the collected SAF/UAF fluorescence light simultaneously as two concentric collimated beams. They are separated
29 afterwards toward their respective detector. The constant splitting between two detectors allows the comparison between
30 the signals mentioned before. See the paper by Verders et al. for a detailed description of the optical setup²⁸.

31 3.2. Lipids and peptides handling

32 1,2-dioleoyl-*sn*-glycero-3-phosphocholine (DOPC) and 1,2-Dioleoyl-*sn*-glycero-3-phospho-L-serine (DOPS) in
33 chloroform were used as received (Avanti Polar Lipids). Fluorescently labelled 1,2-dioleoyl-*sn*-glycero-3-
34 phosphoethanolamine powder (DOPE-Atto647; Atto-tec) was diluted in chloroform. A mixture of 65% DOPC / 35%
35 DOPS was used in the SLB, whose protocol had been optimized and already applied to other SLB-peptide studies^{29,63}.
36 When experiments required fluorescent SLB, DOPE-Atto647 was added to the lipids mixture to achieve a mass ratio of
37 1/62500. This amount was determined to give an optimum fluorescence signal with the SAF technique. The following
38 protocol was used for both fluorescent and non-fluorescent SLB. The lipid solution was stirred under nitrogen then left
39 under vacuum (10 mbar) overnight to remove any trace of solvent. Dried lipids were resuspended in degassed “membrane
40 buffer” (NaCl (100 mM), CaCl₂ · 3H₂O (5 mM), Tris (10 mM), pH 7.4; Sigma Aldrich) and extruded at least 20 times
41 through a porous membrane (0.1 μ m pore size) to yield unilamellar vesicles with a homogeneous size distribution. The
42 vesicles solution was then diluted in the membrane buffer to a concentration of 0.1 mg/mL and passed through a circulating
43 flow system (0.25 mL/min) connected to the sample plate. A glass coverslip was glued on this sample plate after cleaning
44 (cycle of Deconex 11, ethanol and Milli-Q water in ultrasonic bath) and O₂ plasma treatment in order to make the coverslip
45 surface more hydrophilic. When the lipid vesicles adsorbed on this coverslip reached a critical concentration, vesicles

1 fused to form a SLB. Non-disrupted vesicles were removed by extensive washing with the membrane buffer. Finally, SLB
2 was let to stabilize for at least one hour with PBS (Sigma Aldrich) before any measurement.

3 Monomeric A β (1-40), A β (1-42), A β (1-40)-Hylite™ Fluor 647 and A β (1-42)-Hylite™ Fluor 647 (Anaspec) were
4 reconstituted in a 1% NH₄OH solution, then immediately diluted in PBS. Non-labelled peptides were aliquoted at a
5 concentration of 1 mg/mL and kept at -20°C until use (before 6 months of aging). Labelled peptides were aliquoted at the
6 desired concentration and kept frozen until use.

7 3.3 Fluorescence measurements

8 Images of fluorescently labelled SLB or peptide were recorded using the custom-made microscope described previously.
9 Both SAF and UAF signals are collected simultaneously. SAF channel only detects photons arising from the interface
10 vicinity (~200 nm) while UAF channel detects photons emitted from the bulk solution (up to ~2.5 μ m) by the use of
11 confocal optics. The sample is constituted of a metal cell plate, whose volume is approximately 200 μ L and samples were
12 kept under constant flow rate of 0.25 mL/min with the desired peptide solution during measurements. Fast scanning of the
13 sample area was performed via remote control of a mechanical moving frame.

14
15 In order to analyze the mobility of the lipids inside the SLB, fluorescence correlation spectroscopy (FCS) was performed
16 in combination with the supercritical angle collection. Briefly, the method consists to measure fluorescence signal
17 fluctuations due to fluorophores motion within a defined detection volume and to correlate its value over an increasing
18 time lap^{30,64}. The radius of the SAF detection volume was calculated to be 550 \pm 50 nm by measuring the intensity profile
19 of fluorescent nanoparticles⁶⁵. The persistence of the signal after an increasing delay was fitted with a 2-dimensional
20 diffusion model⁶⁶. Fitting allowed calculation of a diffusion coefficient (D_L) which quantifies the lateral diffusion of lipid
21 molecules (Equations 3, 4). The following equations introduce two diffusion coefficients (D_a and D_b), either to account
22 for two leaflets moving differently or for errors that occur at higher τ values. These errors arise when the measuring time
23 is too short to compensate all irregularities. However, short measuring time can be necessary when targeting a specific
24 fluorescent aggregate moving along the SLB.

$$25 \quad G(\tau) = a \cdot G_0 \cdot \frac{1}{1+4D_a/\omega_0^2\tau} + (1-a) \cdot G_0 \cdot \frac{1}{1+4D_b/\omega_0^2\tau} \quad (3)$$

$$26 \quad D_L = a \cdot D_a + (1-a) D_b \quad (4)$$

27 Where G is the autocorrelation value, G_0 is the value at the y intercept, τ is the time delay for the autocorrelation and ω_0
28 being the radius of the detection volume. The signal was monitored during 1 minute for every FCS measurement. FCS
29 curves were fitted with a Matlab program coded specifically.

30

31 Abbreviations

32 A β : Amyloid-Beta, FCS : fluorescence correlation spectroscopy, PBS : phosphate buffer saline, SAF : supercritical
33 angle fluorescence, SLB : supported lipid bilayer, UAF : undercritical angle fluorescence.

34

35 Authors information

36 Valentin Dubois :

37 valentin.dubois@chem.uzh.ch

38 Department of Chemistry, University of Zürich, Wintherthurerstrasse 190, CH-8057 Zürich, Switzerland

39 Diana Serrano :

40 diana.serrano@chimieparistech.psl.eu

41 Stefan Seeger :

1 sseeger@chem.uzh.ch
2 Department of Chemistry, University of Zürich, Winterthurerstrasse 190, CH-8057 Zürich, Switzerland

3 **Acknowledgment**

4 This work was supported by the Swiss National Science Foundation and the University of Zurich.

6 **Supporting informations**

8 S1. SAF imaging of the adsorption of A β on SLB during the short-time adsorption or initial incubation time.

9 S2. SAF imaging of the adsorption of A β on bare glass slide or SLB.

10 S3. SAF imaging of the adsorption of A β on bare glass slide or SLB (2).

11 S4. SAF and UAF imaging of two types of fluorescent SLB after incubation with A β .

12 S5. FCS curves of fluorescent SLB incubated with 50 μ M A β (1-40).

13 S6. FCS curves of fluorescent A β aggregates (10 μ M) incubated on SLB.

14

15 **REFERENCES**

16 1. Dinner, A. R.; Šali, A.; Smith, L. J.; Dobson, C. M.; Karplus, M. (2000) Understanding protein folding via free-energy
17 surfaces from theory and experiment. *Trends in Biochemical Sciences*, 25, 331–339, DOI: 10.1016/S0968-
18 0004(00)01610-8.

19 2. Dobson, C. M. (2003) Protein folding and misfolding. *Nature*, 426, 884–890, DOI: 10.1038/nature02261.

20 3. Clark, P. L. (2004) Protein folding in the cell: Reshaping the folding funnel. *Trends in Biochemical Sciences*, 29, 527–
21 534, DOI: 10.1016/j.tibs.2004.08.008.

22 4. Thomas, P. J.; Qu, B.-H.; Pedersen, P. L. (1995) Defective protein folding as a basis of human disease. *Trends in*
23 *Biochemical Sciences*, 20, 456–459, DOI: 10.1016/S0968-0004(00)89100-8.

24 5. Sunde, M.; Serpell, L. C.; Bartlam, M.; Fraser, P. E.; Pepys, M. B.; Blake, C. C. (1997) Common core structure of
25 amyloid fibrils by synchrotron X-ray diffraction. *Journal of molecular biology*, 273, 729–739, DOI:
26 10.1006/jmbi.1997.1348.

27 6. Jahn, T. R.; Makin, O. S.; Morris, K. L.; Marshall, K. E.; Tian, P.; Sikorski, P.; Serpell, L. C. (2010) The common
28 architecture of cross-beta amyloid. *Journal of molecular biology*, 395, 717–727, DOI: 10.1016/j.jmb.2009.09.039.

29 7. A. S. Cohen, E. Calkins. (1959) Electron microscopic observation on a fibrous component in amyloid of diverse
30 origins. *Nature*, 183, 1202–1203.

31 8. Peter T. Lansbury, JR. (1999) Evolution of amyloid: What normal protein folding may tell us about fibrillogenesis and
32 disease. *Proc. Natl. Acad. Sci. USA*, 96, 3342–3344.

33 9. Masters, C. L.; Simms, G.; Weinman, N. A.; Multhaup, G.; McDonald, B. L.; Beyreuther, K. (1985) Amyloid plaque
34 core protein in Alzheimer disease and Down syndrome. *Proceedings of the National Academy of Sciences*, 82, 4245–
35 4249, DOI: 10.1073/pnas.82.12.4245.

36 10. O'Brien, R. J.; Wong, P. C. (2011) Amyloid precursor protein processing and Alzheimer's disease. *Annual review of*
37 *neuroscience*, 34, 185–204, DOI: 10.1146/annurev-neuro-061010-113613.

38 11. Muresan, V.; Ladescu Muresan, Z. (2015) Amyloid-beta precursor protein: Multiple fragments, numerous transport
39 routes and mechanisms. *Experimental cell research*, 334, 45–53, DOI: 10.1016/j.yexcr.2014.12.014.

- 1 12. Lee, J. P.; Stimson, E. R.; Ghilardi, J. R.; Mantyh, P. W.; Lu, Y.-A.; Felix, A. M.; Llanos, W.; Behbin, A.;
2 Cummings, M. (1995) ¹H NMR of A β . Amyloid Peptide Congeners in Water Solution. Conformational Changes
3 Correlate with Plaque Competence. *Biochemistry*, 34, 5191–5200, DOI: 10.1021/bi00015a033.
- 4 13. Tomaselli, S.; Esposito, V.; Vangone, P.; van Nuland, N. A. J.; Bonvin, A. M. J. J.; Guerrini, R.; Tancredi, T.;
5 Temussi, P. A.; Picone, D. (2006) The alpha-to-beta conformational transition of Alzheimer's A β -(1-42) peptide in
6 aqueous media is reversible: A step by step conformational analysis suggests the location of beta conformation seeding.
7 *Chembiochem : a European journal of chemical biology*, 7, 257–267, DOI: 10.1002/cbic.200500223.
- 8 14. Giacomelli, C. E.; Norde, W. (2005) Conformational changes of the amyloid beta-peptide (1-40) adsorbed on solid
9 surfaces. *Macromolecular bioscience*, 5, 401–407, DOI: 10.1002/mabi.200400189.
- 10 15. Caughey, B.; Lansbury, P. T. (2003) Protofibrils, pores, fibrils, and neurodegeneration: Separating the responsible
11 protein aggregates from the innocent bystanders. *Annual review of neuroscience*, 26, 267–298, DOI:
12 10.1146/annurev.neuro.26.010302.081142.
- 13 16. Lambert, M. P.; Barlow, A. K.; Chromy, B. A.; Edwards, C.; Freed, R.; Liosatos, M.; Morgan, T. E.; Rozovsky, I.;
14 Trommer, B.; Viola, K. L. et al. (1998) Diffusible, nonfibrillar ligands derived from A 1-42 are potent central nervous
15 system neurotoxins. *Proceedings of the National Academy of Sciences*, 95, 6448–6453, DOI: 10.1073/pnas.95.11.6448.
- 16 17. Näslund, J. (2000) Correlation Between Elevated Levels of Amyloid β -Peptide in the Brain and Cognitive Decline.
17 *JAMA*, 283, 1571, DOI: 10.1001/jama.283.12.1571.
- 18 18. Smith, D. G.; Cappai, R.; Barnham, K. J. (2007) The redox chemistry of the Alzheimer's disease amyloid beta
19 peptide. *Biochimica et biophysica acta*, 1768, 1976–1990, DOI: 10.1016/j.bbamem.2007.02.002.
- 20 19. Ian V. J. Murray, Michael E. Sindoni, and Paul H. Axelsen. (2005) Promotion of Oxidative Lipid Membrane Damage
21 by Amyloid β Proteins. *Biochemistry*, 44, 12606–12613.
- 22 20. Sasahara, K.; Morigaki, K.; Shinya, K. (2013) Effects of membrane interaction and aggregation of amyloid β -peptide
23 on lipid mobility and membrane domain structure. *Physical chemistry chemical physics : PCCP*, 15, 8929–8939, DOI:
24 10.1039/c3cp44517h.
- 25 21. M. Kawahara, N. Arispe, Y. Kuroda, and E. Rojas. (1997) Alzheimer's Disease Amyloid (8-Protein Forms Zn²⁺
26 Sensitive, Cation-Selective Channels Across Excised Membrane Patches from Hypothalamic Neurons. *Biophysical*
27 *journal*, 73, 67–75.
- 28 22. Sciacca, Michele F M; Kotler, S. A.; Brender, J. R.; Chen, J.; Lee, D.-k.; Ramamoorthy, A. (2012) Two-step
29 mechanism of membrane disruption by A β through membrane fragmentation and pore formation. *Biophysical journal*,
30 103, 702–710, DOI: 10.1016/j.bpj.2012.06.045.
- 31 23. Khan, M. S.; Dosoky, N. S.; Williams, J. D. (2013) Engineering lipid bilayer membranes for protein studies.
32 *International journal of molecular sciences*, 14, 21561–21597, DOI: 10.3390/ijms141121561.
- 33 24. Czogalla, A.; Grzybek, M.; Jones, W.; Coskun, U. (2014) Validity and applicability of membrane model systems for
34 studying interactions of peripheral membrane proteins with lipids. *Biochimica et biophysica acta*, 1841, 1049–1059,
35 DOI: 10.1016/j.bbalip.2013.12.012.
- 36 25. Richter, R. P.; Berat, R.; Brisson, A. R. (2006) Formation of solid-supported lipid bilayers: An integrated view.
37 *Langmuir : the ACS journal of surfaces and colloids*, 22, 3497–3505, DOI: 10.1021/la052687c.
- 38 26. J. Enderlein, T. Ruckstuhl, and S. Seeger. (1999) Highly efficient optical detection of surface-generated fluorescence.
39 *Appl. Opt.*, 38, 724–732.
- 40 27. T. Ruckstuhl, D. Verdes. (2004) Supercritical angle fluorescence (SAF) microscopy. *Optic express*, 12, 4246–4254.

- 1 28. D. Verdes, T. Ruckstuhl, S. Seeger. (2007) Parallel two-channel near- and far-field fluorescence microscopy. *J.*
2 *Biomed. Opt.* 12(3).
- 3 29. Reynolds, N. P.; Soragni, A.; Rabe, M.; Verdes, D.; Liverani, E.; Handschin, S.; Riek, R.; Seeger, S. (2011)
4 Mechanism of membrane interaction and disruption by α -synuclein. *Journal of the American Chemical Society*, 133,
5 19366–19375, DOI: 10.1021/ja2029848.
- 6 30. Ries, J.; Ruckstuhl, T.; Verdes, D.; Schwille, P. (2008) Supercritical angle fluorescence correlation spectroscopy.
7 *Biophysical journal*, 94, 221–229, DOI: 10.1529/biophysj.107.115998.
- 8 31. Joseph T. Jarrett, Elizabeth P. Berger, and Peter T. Lansbury, Jr. (1993) The Carboxy Terminus of the Amyloid
9 Protein Is Critical for the Seeding of Amyloid Formation: Implications for the Pathogenesis of Alzheimer's Disease.
10 *Biochemistry*, 32, 4693–4697.
- 11 32. Esbjörner, E. K.; Chan, F.; Rees, E.; Erdelyi, M.; Luheshi, L. M.; Bertoncini, C. W.; Kaminski, C. F.; Dobson, C. M.;
12 Kaminski Schierle, G. S. (2014) Direct observations of amyloid β self-assembly in live cells provide insights into
13 differences in the kinetics of A β (1-40) and A β (1-42) aggregation. *Chemistry & biology*, 21, 732–742, DOI:
14 10.1016/j.chembiol.2014.03.014.
- 15 33. Quinn, S. D.; Dalgarno, P. A.; Cameron, R. T.; Hedley, G. J.; Hacker, C.; Lucocq, J. M.; Baillie, G. S.; Samuel, I. D.
16 W.; Penedo, J. C. (2014) Real-time probing of β -amyloid self-assembly and inhibition using fluorescence self-quenching
17 between neighbouring dyes. *Molecular bioSystems*, 10, 34–44, DOI: 10.1039/c3mb70272c.
- 18 34. Rabe, M.; Verdes, D.; Zimmermann, J.; Seeger, S. (2008) Surface organization and cooperativity during nonspecific
19 protein adsorption events. *The journal of physical chemistry. B*, 112, 13971–13980, DOI: 10.1021/jp804532v.
- 20 35. Rabe, M.; Verdes, D.; Seeger, S. (2011) Understanding protein adsorption phenomena at solid surfaces. *Advances in*
21 *colloid and interface science*, 162, 87–106, DOI: 10.1016/j.cis.2010.12.007.
- 22 36. Daly, S. M.; Przybycien, T. M.; Tilton, R. D. (2003) Coverage-Dependent Orientation of Lysozyme Adsorbed on
23 Silica. *Langmuir*, 19, 3848–3857, DOI: 10.1021/la026690x.
- 24 37. Wertz, C. F.; Santore, M. M. (2002) Adsorption and Reorientation Kinetics of Lysozyme on Hydrophobic Surfaces.
25 *Langmuir*, 18, 1190–1199, DOI: 10.1021/la0108813.
- 26 38. B. Soreghan, J. Kosmoski, C. Glabe. (1994) Surfactant Properties of Alzheimer's ABeta-Peptides and the
27 Mechanism of Amyloid Aggregation. *The Journal of biological chemistry*, 269.
- 28 39. Liu, Y.; Shen, L. (2008) From Langmuir kinetics to first- and second-order rate equations for adsorption. *Langmuir :*
29 *the ACS journal of surfaces and colloids*, 24, 11625–11630, DOI: 10.1021/la801839b.
- 30 40. Matsuzaki, K. (2007) Physicochemical interactions of amyloid beta-peptide with lipid bilayers. *Biochimica et*
31 *biophysica acta*, 1768, 1935–1942, DOI: 10.1016/j.bbamem.2007.02.009.
- 32 41. Ariga, T.; Kobayashi, K.; Hasegawa, A.; Kiso, M.; Ishida, H.; Miyatake, T. (2001) Characterization of high-affinity
33 binding between gangliosides and amyloid beta-protein. *Archives of biochemistry and biophysics*, 388, 225–230, DOI:
34 10.1006/abbi.2001.2304.
- 35 42. D. L. Miller, I. A. Papayannopoulos, J. Styles. (1993) Peptide Composition of the Cerebrovascular and Senile Plaque
36 Core Amyloid Deposits of Alzheimer disease. *Archives of biochemistry and biophysics*, 301.
- 37 43. T. Iwatsubo, A. Odaka, N. Suzuki. (1994) Visualization of AB42(43) and AB40 in Senile Plaques with End-Specific
38 AB Monoclonals: Evidence that an Initially Deposited Species Is AB42(43). *Neuron*, 13, 45–53.
- 39 44. A. Quist, I. Doudevski, H. Lin, R. Azimova. (2005) Amyloid ion channels: A common structural link for protein-
40 misfolding disease. *PNAS*, 102, 10427–10432.

- 1 45. Karran, E.; Mercken, M.; Strooper, B. de. (2011) The amyloid cascade hypothesis for Alzheimer's disease: an
2 appraisal for the development of therapeutics. *Nature reviews. Drug discovery*, 10, 698–712, DOI: 10.1038/nrd3505.
- 3 46. Daniel Axelrod. (1983) Lateral Motion of Membrane Proteins and Biological Function. *Membrane Biology*, 75, 1–
4 10.
- 5 47. Nicolson, G. L. (2014) The Fluid-Mosaic Model of Membrane Structure: still relevant to understanding the structure,
6 function and dynamics of biological membranes after more than 40 years. *Biochimica et biophysica acta*, 1838, 1451–
7 1466, DOI: 10.1016/j.bbamem.2013.10.019.
- 8 48. Przybylo, M.; Sýkora, J.; Humpolíckova, J.; Benda, A.; Zan, A.; Hof, M. (2006) Lipid diffusion in giant unilamellar
9 vesicles is more than 2 times faster than in supported phospholipid bilayers under identical conditions. *Langmuir : the*
10 *ACS journal of surfaces and colloids*, 22, 9096–9099, DOI: 10.1021/la061934p.
- 11 49. Scomparin, C.; Lecuyer, S.; Ferreira, M.; Charitat, T.; Tinland, B. (2009) Diffusion in supported lipid bilayers:
12 influence of substrate and preparation technique on the internal dynamics. *The European physical journal. E, Soft matter*,
13 28, 211–220, DOI: 10.1140/epje/i2008-10407-3.
- 14 50. Ding, H.; Schauerte, J. A.; Steel, D. G.; Gafni, A. (2012) β -Amyloid (1-40) peptide interactions with supported
15 phospholipid membranes: a single-molecule study. *Biophysical journal*, 103, 1500–1509, DOI:
16 10.1016/j.bpj.2012.08.051.
- 17 51. Khachaturian, Z. S. (1987) Hypothesis on the Regulation of Cytosol Calcium Concentration and the Aging Brain.
18 *Neurobiology of Aging*, 8, 345–346, DOI: 10.1016/0197-4580(87)90073-X.
- 19 52. M. P. Mattson, B. Cheng, D. Davis, K. Bryant, I. Lieberburg, and R. E. Rydel. (1992) B-Amyloid Peptides
20 Destabilize Calcium Homeostasis and Render Human Cortical Neurons Vulnerable to Excitotoxicity. *the journal of*
21 *neuroscience*, 376–389.
- 22 53. Arispe, N., Pollard, H. B. & Rojas. (1993) Giant multilevel cation channels formed by Alzheimer disease amyloid
23 beta-protein [A beta (1-40)] in bilayer membranes. *Proc. Nati. Acad. Sci. USA*, 90, 567–571.
- 24 54. Kagan, B. L.; Azimov, R.; Azimova, R. (2004) Amyloid peptide channels. *The Journal of membrane biology*, 202,
25 1–10, DOI: 10.1007/s00232-004-0709-4.
- 26 55. H. W. Querfurth, D. J. Selkoe. (1994) Calcium Ionophore Increases Amyloid .beta. Peptide Production by Cultured
27 Cells. *Biochemistry*, 33, 4550–4561.
- 28 56. Itkin, A.; Dupres, V.; Dufrière, Y. F.; Bechinger, B.; Ruyschaert, J.-M.; Raussens, V. (2011) Calcium ions promote
29 formation of amyloid β -peptide (1-40) oligomers causally implicated in neuronal toxicity of Alzheimer's disease. *PloS*
30 *one*, 6, e18250, DOI: 10.1371/journal.pone.0018250.
- 31 57. Yu, X.; Zheng, J. (2012) Cholesterol promotes the interaction of Alzheimer β -amyloid monomer with lipid bilayer.
32 *Journal of molecular biology*, 421, 561–571, DOI: 10.1016/j.jmb.2011.11.006.
- 33 58. Hortschansky, P.; Schroeckh, V.; Christopeit, T.; Zandomenighi, G.; Fändrich, M. (2005) The aggregation kinetics
34 of Alzheimer's beta-amyloid peptide is controlled by stochastic nucleation. *Protein science : a publication of the Protein*
35 *Society*, 14, 1753–1759, DOI: 10.1110/ps.041266605.
- 36 59. Lockhart, C.; Klimov, D. K. (2015) Calcium enhances binding of A β monomer to DMPC lipid bilayer. *Biophysical*
37 *journal*, 108, 1807–1818, DOI: 10.1016/j.bpj.2015.03.001.
- 38 60. Lau, T.-L.; Ambroggio, E. E.; Tew, D. J.; Cappai, R.; Masters, C. L.; Fidelio, G. D.; Barnham, K. J.; Separovic, F.
39 (2006) Amyloid-beta peptide disruption of lipid membranes and the effect of metal ions. *Journal of molecular biology*,
40 356, 759–770, DOI: 10.1016/j.jmb.2005.11.091.

- 1 61. Terzi, E.; Hölzemann, G.; Seelig, J. (1997) Interaction of Alzheimer beta-amyloid peptide(1-40) with lipid
2 membranes. *Biochemistry*, 36, 14845–14852, DOI: 10.1021/bi971843e.
- 3 62. Winterflood, C. M.; Ruckstuhl, T.; Verdes, D.; Seeger, S. (2010) Nanometer axial resolution by three-dimensional
4 supercritical angle fluorescence microscopy. *Physical review letters*, 105, 108103, DOI:
5 10.1103/PhysRevLett.105.108103.
- 6 63. Rabe, M.; Soragni, A.; Reynolds, N. P.; Verdes, D.; Liverani, E.; Riek, R.; Seeger, S. (2013) On-surface aggregation
7 of α -synuclein at nanomolar concentrations results in two distinct growth mechanisms. *ACS chemical neuroscience*, 4,
8 408–417, DOI: 10.1021/cn3001312.
- 9 64. Elson, E. L.; Magde, D. (1974) Fluorescence correlation spectroscopy. I. Conceptual basis and theory. *Biopolymers*,
10 13, 1–27, DOI: 10.1002/bip.1974.360130102.
- 11 65. C. M. Winterflood. PhD. Thesis. University of Zürich.
- 12 66. Heinemann, F.; Betaneli, V.; Thomas, F. A.; Schwille, P. (2012) Quantifying lipid diffusion by fluorescence
13 correlation spectroscopy: a critical treatise. *Langmuir : the ACS journal of surfaces and colloids*, 28, 13395–13404, DOI:
14 10.1021/la302596h.
- 15
- 16
- 17